Case Report

Intraoperative mapping of expressive language cortex using passive real-time electrocorticography

AmiLyn M. Taplin [a], Adriana de Pesters [b,c], Peter Brunner [b,d], Dora Hermes [e], John C. Dalfino [a], Matthew A. Adamo [a], Anthony L. Ritaccio [d], Gerwin Schalk [b,c,d,*]

[a] Department of Neurosurgery, Albany Medical College, Albany, NY, USA
[b] National Center for Adaptive Neurotechnologies, Wadsworth Center, New York State Department of Health, Albany, NY, USA
[c] Department of Biomedical Sciences, State University of New York at Albany, Albany, NY, USA
[d] Department of Neurology, Albany Medical College, Albany, NY, USA
[e] Department of Psychology, Stanford University, Stanford, CA, USA

ABSTRACT

In this case report, we investigated the utility and practicality of passive intraoperative functional mapping of expressive language cortex using high-resolution electrocorticography (ECoG). The patient presented here experienced new-onset seizures caused by a medium-grade tumor in very close proximity to expressive language regions. In preparation of tumor resection, the patient underwent multiple functional language mapping procedures. We examined the relationship of results obtained with intraoperative high-resolution ECoG, extraoperative ECoG utilizing a conventional subdural grid, extraoperative electrical cortical stimulation (ECS) mapping, and functional magnetic resonance imaging (fMRI). Our results demonstrate that intraoperative mapping using high-resolution ECoG is feasible and, within minutes, produces results that are qualitatively concordant to those achieved by extraoperative mapping modalities. They also suggest that functional language mapping of expressive language areas with ECoG may prove useful in many intraoperative conditions given its time efficiency and safety. Finally, they demonstrate that integration of results from multiple functional mapping techniques, both intraoperative and extraoperative, may serve to improve the confidence in or precision of functional localization when pathology encroaches upon eloquent language cortex.

1. Introduction

Precise localization of eloquent cortex facilitates optimal surgical outcomes in patients with tumors, epileptogenic foci, or vascular abnormalities. Operative planning balances removal of pathologic tissue that portends specific symptomatic morbidity with preservation of the eloquent cortex necessary for maintaining an acceptable quality of life. Historically, functional mapping has been conducted primarily with electrical cortical stimulation (ECS) [1,2], but also with functional magnetic resonance imaging (fMRI) [3], extraoperative (chronic) electrocorticography (ECoG) [4–6], electroencephalography (EEG) [7,8], magnetoencephalography (MEG) [9], or positron emission tomography (PET) [10]. Each of these techniques carries inherent limitations that impede widespread application in the approximately 111,000 patients that undergo brain surgery for removal of a brain tumor or epileptogenic focus each year [11].

Electrical cortical stimulation currently stands as the 'gold standard' for functional mapping. The technique is procedurally simple and has a relatively low cost. Its most notable limitation remains the extensive amount of time required to conduct the procedure. This issue becomes particularly apparent when ECS is performed under the time constraints of an awake craniotomy in the operating room. In addition, active stimulation of the brain with ECS can provoke after-discharges and seizures. Iatrogenic seizures can increase patient morbidity as well as the duration of mapping.

Functional MRI is another mapping technique that has garnered avid attention recently. Its primary advantage is its noninvasive nature and excellent spatial resolution. However, it only indirectly evaluates neuronal activity by measuring task-related BOLD changes [12,13]. Highly vascularized malignant tumors can alter cerebrovascular hemodynamics and BOLD patterns; hence, they may not accurately reflect eloquent cortical function [14,15]. Furthermore, clinical application of fMRI for real-time mapping is hindered by the extensive time and expertise required for the requisite post hoc analyses.

Electrocorticography, another passive functional mapping modality, is emerging and currently undergoing significant investigation. This technique identifies changes in cortical activity in response to specific

* Corresponding author at: National Center for Adaptive Neurotechnologies, Wadsworth Center, NYS Dept. of Health, Center for Medical Science 2003, 150 New Scotland Avenue, Albany, NY 12208, USA. Tel.: +1 518 486 2559; fax: +1 518 486 4910.
E-mail address: gschalk@neurotechcenter.org (G. Schalk).

language, motor, or cognitive tasks. Recording these changes in cortical activity does not require application of electrical impulses to induce an effect, thereby eliminating the risk of seizures. Electrocorticography changes in the broadband gamma range (>60 Hz) are of particular relevance in this context of functional mapping [16]. They represent the average firing rate of neurons directly underneath the electrodes [17–19] and are highly task-specific [20]. They have also been shown to correlate well with the blood oxygen-level dependent (BOLD) response detected by fMRI [21]. Recent advances in neural signal acquisition [22,23] and processing [24] have provided the methodological basis for mapping of cortical activity in real time [25]. Despite these advances, ECoG-based mapping predominantly occurs in the epilepsy monitoring unit, remaining as an extraoperative endeavor. With few exceptions [26,27], the practicality and potential value of ECoG-based mapping in the operating room remains largely unexplored, particularly with investigation using high-resolution recordings. In this case report, we test the feasibility of intraoperative mapping using real-time ECoG.

In summary, accurate and practical functional mapping in the operating room still faces challenges in contemporary practice. Mapping based on ECoG promises rapidity, a high spatial specificity, and no increased morbidity. Combining data obtained from ECS, ECoG, and fMRI can provide complementary information that may be useful for surgical planning of complex cases. In the present case, we mapped expressive language function with ECoG using a high-density grid during an awake craniotomy. We confirmed the location of frontal language areas extraoperatively using fMRI, standard ECS mapping, and ECoG mapping. We integrated and visualized the results, producing highly detailed functional maps. These composite results suggested qualitative concordance of eloquent expressive language cortex across the different mapping modalities.

2. Case report

2.1. Initial presentation

The patient was a 33-year-old male who presented after a motor vehicle accident while experiencing a first time seizure. The patient had a computerized tomography (CT) scan as part of his initial evaluation that suggested a hypodensity in the left frontal lobe. Magnetic resonance (MR) imaging revealed a nonenhancing left frontal mass (Fig. 1, left), and MR spectroscopy characteristics supported a low-to-medium grade tumor. Given the anatomic location of the tumor's proximity to presumed Broca's area, the patient underwent fMRI and diffusion tensor

imaging (DTI). The fMRI confirmed the close relationship of the tumor to Broca's area (within 3–5 mm) with verb generation and object naming tasks (p < 0.05, family-wise error correction) (Fig. 1, right).

The patient did not have any further seizures after the initiation of levetiracetam, and he remained neurologically intact without any focal deficits or aphasia. To comprehensively evaluate expressive language cortex for an optimal postoperative outcome, the patient elected to pursue a two-staged brain mapping procedure with the use of subdural grids and ECS. Prior to surgery, the patient had neuropsychological testing for baseline evaluation using the Wechsler Adult Intelligence Scale WAIS-IV [28]. The patient gave informed consent for a protocol that was reviewed and approved by the institutional review board of Albany Medical College as well as the US Army Medical Research and Materiel Command.

2.2. Stage 1 operation

The patient underwent implantation of an 8 × 8 cm silicon subdural grid embedded with 64 platinum iridium electrodes of 4 mm diameter (2.3 mm exposed) and interelectrode distance of 1 cm [PMT, Chanhassen, MN] (Fig. 2, panels A and B). Contacts 1, 2, and 9 were removed for better contour along the cortical surface. Contact 57 was located most anteriorly, contact 64 most superiorly, and contact 8 most posteriorly (Fig. 3). A four-contact electrode strip was placed on the skull to provide a ground for the clinical monitoring system. The patient tolerated the first stage well and was connected to a Nihon-Kohden Neurofax video-EEG monitoring system [Tokyo, Japan] that continuously recorded ECoG signals as well as accompanying clinical behavior. To ensure integrity of clinical data collection, passive splitter connectors simultaneously provided ECoG signals to eight optically isolated and synchronized 16-channel g.USBamp amplifier/digitizer units (g.tec, Graz, Austria) with signal sampling at 1200 Hz. Clinical review of ECoG signals identified frequent left frontal spikes and spike and wave discharges at contact 23.

2.3. Clinical mapping

On postoperative day 2, the patient underwent extraoperative functional cortical mapping in the epilepsy monitoring unit (EMU) with ECoG and ECS procedures. For ECoG mapping, the broadband gamma signal at each contact location was measured and compared between rest and task epochs to establish the statistical difference across these tasks (see [29] for detailed methodology). The patient first rested
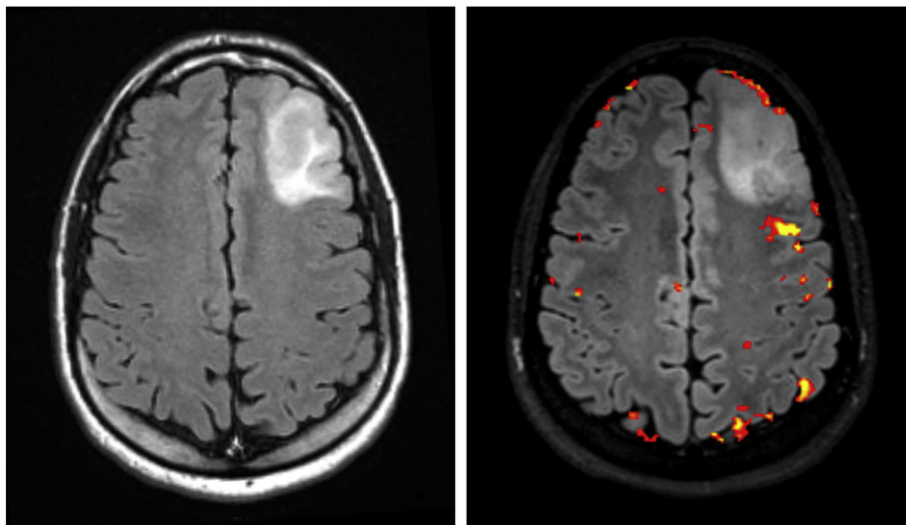

Fig. 1. (Left) Preoperative axial T2-weighted FLAIR MR image on 1.5 T magnet demonstrating a tumor in the anterior left frontal lobe. (Right) Preoperative fMRI on 3 T magnet indicating proximity of tumor to Broca's area, within 3–5 mm on postprocessed images.
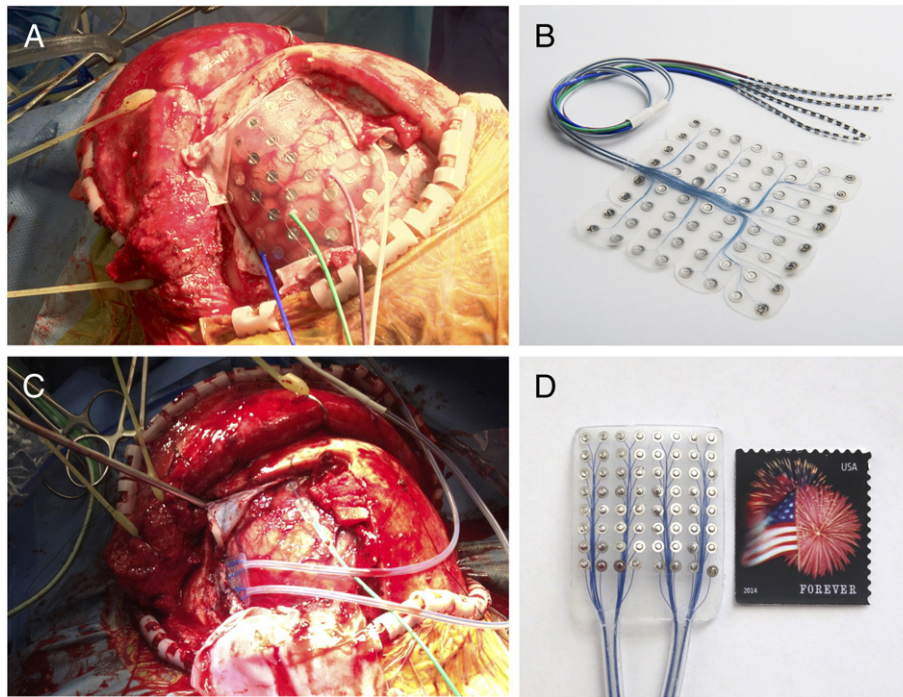
Fig. 2. (A) Intraoperative photograph of left frontal lobe exposure with standard 64-contact subdural grid. (B) Example of subdural grid used during the case, courtesy of PMT Corporation. (C) Intraoperative photograph of high-density grid placed over eloquent cortex previously identified by the standard grid. (D) High-density 64-contact silicon grid used during the case.

quietly for six minutes to establish a model of baseline ECoG activity. The patient then performed several repetitive motor and language tasks as instructed by visual cues: 1) solve Rubik's cube, 2) shrug shoulders, 3) stick out tongue, 4) purse lips, 5) listen to a narrative, 6) generate verbs, and 7) imagine generating verbs. This ECoG paradigm identified electrode contacts 11 and 12 (Fig. 3) as expressive language nodes within a few minutes.

For the ECS procedure, we used a digital Grass S12X stimulator with built-in stimulus isolation and constant current circuitry [Grass Technologies, Warwick, RI] to stimulate pairs of electrodes using a pulse duration of 0.3 ms, variable frequencies between 20 and 50 Hz, current ranging from 1 to 15 mA, and train durations of 5 s. Bipolar and monopolar modalities were assessed with increasing current until

after-discharges or a functional response was elicited, or the maximum amount of current was reached at 15 mA. Stimulation of contacts 11 and 12 with 10 mA at 20 Hz rendered complete speech arrest, indicating eloquence. These nodes were confirmed on four separate occasions throughout the procedure. Oral motor function was also identified. An electrographic seizure was elicited with stimulation of contacts 23 and 41 during mapping; the patient was treated with 2 mg IV lorazepam, 1000 mg IV levetiracetam, and 500 mg fosphenytoin. Further mapping was delayed for approximately 90 min due to the stimulus-induced seizure and subsequent postictal period.

2.4. Stage 2 operation

Five days after the initial subdural grid implantation, the patient returned to the operating room for the second stage. Once the previous craniotomy flap was reopened and the cortical surface was exposed with good hemostasis, the standard subdural grid was replaced with a high-density 64-contact silicon grid (PMT Corp., Chanhassen, MN), measuring 2.5 × 2.5 cm embedded with platinum iridium electrodes of 2 mm diameter (1 mm exposed) and with an interelectrode distance of 3 mm (Fig. 2, panels C and D). To further refine the boundary of expressive language function, this high-density grid covered only the language cortex previously identified by extraoperative ECoG and ECS mapping. The patient was reversed from anesthesia for awake passive mapping. Within minutes, intraoperative ECoG mapping using verb generation and word repetition identified the most significant ECoG changes at locations corresponding to contacts 11 and 12 of the original standard subdural grid. These locations were outlined for preservation. The patient tolerated the procedure very well and was induced back under anesthesia for the remainder of the surgery.

2.5. Postoperative course

The patient experienced an excellent recovery and had very mild issues of transient confusion. Permanent pathology revealed focal anaplasia WHO III in the setting of diffuse fibrillary astrocytoma WHO II. The patient had adjuvant chemoradiation therapy. Postoperative
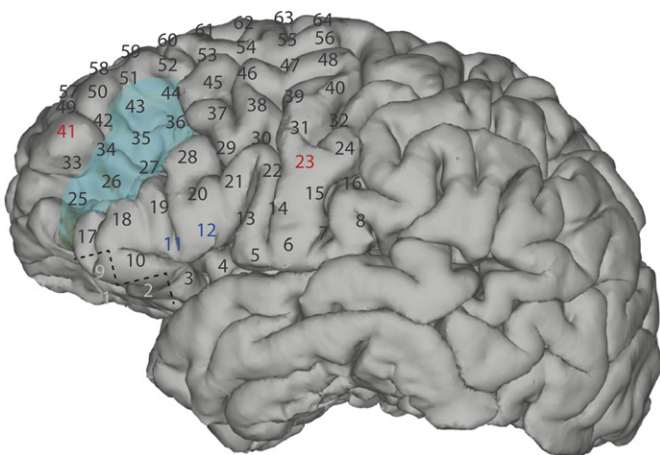

Fig. 3. Numbers represent electrode contacts of the standard subdural grid coverage. The tumor margins are displayed as light blue. Electrical stimulation of contacts 11 and 12 (dark blue) caused speech arrest in Broca's area. Electrical stimulation of contacts 23 and 41 (red) caused an electrographic seizure; contacts 1, 2 and 9 (light gray) were removed for better contour along the cortical surface.

neuropsychological testing (at 1 year) demonstrated a 28% decline in verbal fluency and a slight decrement in recent memory/new learning (although still within high average range). Surveillance imaging over 28 months has yet to demonstrate recurrence.

2.6. Coregistration of mapping techniques

The main results presented in this case report are the mapping results from fMRI, ECS, and extra- and intraoperative ECoG. They are summarized in Fig. 4. For fMRI data acquisition, preoperative scans were acquired on a Philips Ingenia 3 T scanner with an echo planar imaging (EPI) sequence (80 scans, acquisition voxel size 3 mm isotropic, repetition time (TR) 3 s, echo time (TE) 30 ms, flip angle 90°, field of view (FOV) 237 mm). Functional MRI data were preprocessed and analyzed using statistical parametric mapping software (SPM8, http://www.fil.ion.ucl.ac.uk/spm). Images were realigned and coregistered with an anatomical scan using normalized mutual information [30]. Statistical analyses were performed on a single-subject basis, and therefore, no smoothing was applied. A general linear model was estimated with one regressor for verb generation (a 15 s box car for verb generation blocks convolved with a standard hemodynamic response function); data were corrected for low frequency drifts by a 128 s high pass filter and corrected for serial correlations with a first-order autoregressive model. Functional MRI results were rendered on the surface of the cortex (Fig. 4, left) in similar manner as before [21,31], plotting any activation up to 8 mm below the surface. Functional MRI activity was plotted with a threshold of $t(150) > 5.51$, $p_{FWEcorrected} < 0.05$.

We created a three-dimensional patient-specific cortical surface brain model by submitting the preoperative high resolution MRI scans to Freesurfer (http://surfer.nmr.mgh.harvard.edu). We identified the stereotactic coordinates of the standard subdural grid using SPM8

software (http://www.fil.ion.ucl.ac.uk/spm/) and custom MATLAB scripts (The MathWorks Inc., Natick, MA), which coregistered the MRI scans with the postoperative CT scans. The high-density subdural grid contacts were coregistered with those of the standard subdural grid using scalp fiducial markers, an intraoperative neuronavigation system (BrainLab AG, Feldkirchen, Germany), and novel custom software [32]. The electrode locations were then projected onto a three-dimensional brain model and custom NeuralAct [33] software (Fig. 4, right) to render activation maps of corresponding ECoG activity.

3. Discussion

This case report represents the first application of high-resolution ECoG-based mapping in the operating room and demonstrates one of the most comprehensive examples of multimodal functional mapping to date. We mapped expressive language function in a patient using four different modalities: ECS, extraoperative ECoG, intraoperative ECoG, and fMRI. Recent technological advances enabled us to combine the results into an informative display that facilitated comparison across modalities. This comparison suggested qualitatively concordant functional language maps. In particular, ECS and extraoperative ECoG delineated identical critical language nodes using a standardized grid coordinate system. The same locations were confirmed with intraoperative high-resolution ECoG. Thus, our results highlight the value of passive ECoG-based mapping in the extraoperative as well as the intraoperative environment.

Electrical cortical stimulation currently represents the "gold standard" for functional cortical mapping even in the absence of standardization and validation by randomized controlled trials. Given the recent technological advances, ECoG-based mapping offers the potential for similar precision but with a greater safety profile, better patient
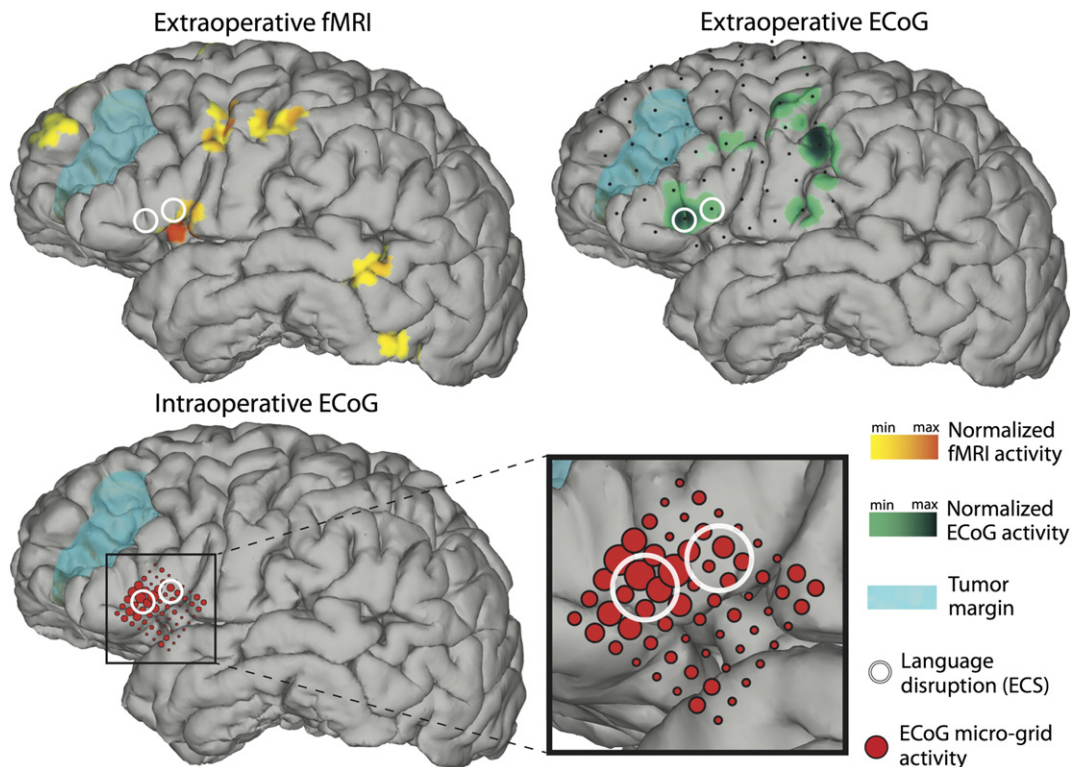

Fig. 4. (Top left) Functional MRI showing increased BOLD activity (shown in yellow and orange) in Broca's area, as well as auditory/Wernicke's area, precentral gyrus, supplementary motor/premotor cortex and prefrontal cortex. ECS (white circles) caused speech arrest in Broca's area, adjacent to increased BOLD activity. (Top right) Small black dots represent electrode contacts of the standard extraoperative subdural grid. Results from extraoperative ECoG-based functional mapping (shown in green) demonstrated increased activity in Broca's area, precentral gyrus, supplementary motor/premotor cortex and postcentral gyrus. (Bottom) Results from intraoperative ECoG-based mapping are shown in red. The diameter of each circle is proportional to the activity under the corresponding electrode contact. The largest circles identify locations that are qualitatively concordant with those from extraoperative ECoG-based and ECS mapping.

tolerability, and faster data acquisition time. Several studies have compared the mapping results of ECoG with those of ECS, reporting sensitivities ranging from 0.43–1.0 and specificities of 0.72–0.94 for sensorimotor mapping [4,5,16,29,34,35]. However, evidence for concordance of ECoG with ECS for language mapping is relatively sparse. In their 2005 study of 13 patients, Sinai et al. reported a sensitivity of 38% and specificity of 78% for language mapping [35]. Miller et al. [36] applied extraoperative ECoG in 7 patients to elucidate cortical areas for expressive and receptive language. They reported a sensitivity of 89% and specificity of 66% for a noun-reading task and a sensitivity of 74% and specificity of 48% for a verb generation task when compared with ECS. A case report of a 13-year-old patient with intractable epilepsy yielded sensitivity of 75% and 90% when using the 'next-neighbor' hypothesis for ECoG compared with ECS mapping for language function [37]. Case reports in the intraoperative environment [26,27] have provided qualitative concordance between ECoG and ECS data, suggesting that ECoG can facilitate more efficient ECS interrogation. Our case reinforces the practical advantage of ECoG for language mapping.

Comparing the concordance of ECS and ECoG proves difficult given the fundamental differences in the approach of lesion-based mapping versus physiologic-based mapping. Electrical cortical stimulation "actively" disrupts cortical networks critical for a particular function and only identifies those subsets of task-related cortical networks whose lesion produces the most severe functional deficits, whereas ECoG "passively" highlights all cortical networks involved with a particular task [38]. Another complicating factor arises from the comparison of a single ECoG(+) site that exhibits a signal change in broadband gamma to an ECS(+) site that is derived from pairwise electrical stimulation. Ultimately, the most important aspect is the relative clinical utility of each method. Establishing clinical utility requires standardized preoperative and postoperative assessments in a large number of patients. For ECoG, such larger assessments do not yet exist.

Electrical cortical stimulation and ECoG each have important limitations for clinical application. Both modalities currently require awake craniotomies or staged procedures and depend entirely on patient comfort and compliance. Staged procedures carry significant financial burden as well as stress associated with a prolonged hospitalization in an unfamiliar environment. The risk of infection increases with implanted materials and duration of implantation. Patients assume all the surgical risks of a second operation. The physical mapping with ECS is time and labor intensive for the clinician and the patient. The appropriate stimulation energy must be determined and then applied to each single grid contact in an organized method. Electrical stimulation can cause pain from activation of dural nociceptive afferents and general cephalalgia [38]. Electrical cortical stimulation can produce after-discharges that may summate into seizures with subsequent postictal periods that can further delay mapping. Finally, ECS may produce inhibitory responses that cannot readily be observed and may have variable propagation of stimulation current due to individual anatomy and procedural differences [29,39]. In our case, the patient did have a seizure that prolonged the mapping time by 1.5 h, increasing total mapping duration to 4.5 h. Passively recorded ECoG incurs less risk of cephalalgia, reduces the risk for iatrogenic seizures, and has dramatically shortened mapping time since it can evaluate cortical activity from all electrodes simultaneously.

As with ECS and ECoG, the concordance between ECS and fMRI varies, with reported sensitivity and specificity measurements for language mapping varying between 59%–100% and 53%–97%, respectively [40–45]. Our case report demonstrated strong concordance between fMRI, ECoG, and ECS for the language sites identified on the pars opercularis but not as well for the language sites on the pars triangularis. Multiple issues can influence this mismatch on the pars triangularis. First, we used a conservative fMRI threshold, and only the most robust sites reached this threshold in the analysis (see Supplementary Fig. 1 that demonstrates BOLD activation in the pars triangularis when a lower threshold is used). Second, blood flow artifacts can obscure the fMRI signal, making it more difficult to measure in certain regions compared with others [14,15]. Lastly, previous fMRI studies often used a battery of language tasks to localize language areas [46], whereas we only evaluated verb generation and word repetition. A more comprehensive battery across modalities may provide better-matched results.

To our knowledge, this is the first instance of using a high-density subdural grid in the intraoperative environment for language mapping. With its superior spatial resolution, we were able to create a highly refined boundary between the tumor and expressive language cortex. These results are encouraging, but important questions are not yet resolved. How does this improved spatial resolution translate into improved patient outcomes? What is the optimal electrode diameter size and interelectrode distance for best spatial resolution that will provide nonredundant recordings [47–49]? At what point will the spatial resolution of high-density subdural grids exceed the operative resolution of neurosurgery with available techniques?

Even with mapping of Broca's area and the specific language nodes, our patient still suffered a 28% decline in verbal fluency at one year. Can we attribute this decline in verbal fluency as a postoperative deficit (as seen in 3–13% of patients with brain tumor who undergo surgery [50–52]) or to that of radiation necrosis potentiated by chemotherapy (that afflicts 2.5–5% of patients [53])? Our patient had undergone formal neuropsychiatric evaluation. Functional limitations or clinical observations (as used in some other studies) would likely have missed these subtle changes.

Functional language mapping during an awake craniotomy remains a challenge. Here, we demonstrate that functional mapping with high-resolution electrocorticography can readily be performed in the intraoperative environment and that its results appear qualitatively concordant with ECS. At this juncture, there is no universal standard of care for functional language mapping. Taking into account the unique strengths and limitations of each modality, no one technique is clearly superior to the others. The rate of investigation into various modalities for functional brain mapping is at its zenith, with the impetus to improve clinical outcomes for patients with epilepsy, tumors, or vascular malformations.

Supplementary data to this article can be found online at http://dx.doi.org/10.1016/j.ebcr.2016.03.003.

Acknowledgments

Disclosure

The authors report no conflict of interest concerning the materials or methods used in this study or the findings specified in this paper.

References

[1] Ojemann GA. Cortical organization of language. J Neurosci 1991;11(8):2281–7.
[2] Penfield W, Boldrey E. Somatic motor and sensory representation in the cerebral cortex of man as studied by electrical stimulation. Brain 1937;60(4):389–443.
[3] Chakraborty A, McEvoy AW. Presurgical functional mapping with functional MRI. Curr Opin Neurol 2008;21(4):446–51.
[4] Crone NE, Miglioretti DL, Gordon B, Sieracki JM, Wilson MT, Uematsu S, et al. Functional mapping of human sensorimotor cortex with electrocorticographic spectral analysis. I. Alpha and beta event-related desynchronization. Brain 1998;121(Pt 12): 2271–99.
[5] Leuthardt EC, Miller K, Anderson NR, Schalk G, Dowling J, Miller J, et al. Electrocorticographic frequency alteration mapping: a clinical technique for mapping the motor cortex. Neurosurgery 2007;60(4 Suppl 2):260–70 [discussion 70-1].
[6] Miller KJ, Leuthardt EC, Schalk G, Rao RP, Anderson NR, Moran DW, et al. Spectral changes in cortical surface potentials during motor movement. J Neurosci 2007; 27(9):2424–32.

[7] Graimann B, Huggins JE, Levine SP, Pfurtscheller G. Visualization of significant ERD/ERS patterns in multichannel EEG and ECoG data. Clin Neurophysiol 2002;113(1):43–7.

[8] Lachaux JP, Rudrauf D, Kahane P. Intracranial EEG and human brain mapping. J Physiol Paris 2003;97(4–6):613–28.

[9] Ganslandt O, Fahlbusch R, Nimsky C, Kober H, Moller M, Steinmeier R, et al. Functional neuronavigation with magnetoencephalography: outcome in 50 patients with lesions around the motor cortex. Neurosurg Focus 1999;6(3):e3.

[10] Bittar RG, Olivier A, Sadikot AF, Andermann F, Comeau RM, Cyr M, et al. Localization of somatosensory function by using positron emission tomography scanning: a comparison with intraoperative cortical stimulation. J Neurosurg 1999;90(3):478–83.

[11] AANS. National Neurosurgical Procedural Statistics, Tech. Rep. American Association of Neurological Surgeons; 2012.

[12] Holodny AI, Schulder M, Liu WC, Maldjian JA, Kalnin AJ. Decreased BOLD functional MR activation of the motor and sensory cortices adjacent to a glioblastoma multiforme: implications for image-guided neurosurgery. AJNR Am J Neuroradiol 1999;20(4):609–12.

[13] Schreiber A, Hubbe U, Ziyeh S, Hennig J. The influence of gliomas and nonglial space-occupying lesions on blood-oxygen-level-dependent contrast enhancement. AJNR Am J Neuroradiol 2000;21(6):1055–63.

[14] Kekhia H, Rigolo L, Norton I, Golby AJ. Special surgical considerations for functional brain mapping. Neurosurg Clin N Am 2011;22(2):111–32.

[15] Tharin S, Golby A. Functional brain mapping and its applications to neurosurgery. Neurosurgery 2007;60(4):185–202.

[16] Crone NE, Miglioretti DL, Gordon B, Lesser RP. Functional mapping of human sensorimotor cortex with electrocorticographic spectral analysis. II. Event-related synchronization in the gamma band. Brain 1998;121(Pt 12):2301–15.

[17] Miller KJ, Sorensen LB, Ojemann JG, den Nijs M. Power-law scaling in the brain surface electric potential. PLoS Comput Biol 2009;5(12), e1000609.

[18] Ray S, Maunsell JHR. Different origins of gamma rhythm and high-gamma activity in macaque visual cortex. PLoS Biol 2011;9(4), e1000610.

[19] Manning JR, Jacobs J, Fried I, Kahana MJ. Broadband shifts in local field potential power spectra are correlated with single-neuron spiking in humans. J Neurosci 2009;29(43):13613–20.

[20] Miller KJ, Honey CJ, Hermes D, Rao RPN, DenNijs M, Ojemann JG. Broadband changes in the cortical surface potential track activation of functionally diverse neuronal populations. Neuroimage 2014;85(Pt 2):711–20.

[21] Hermes D, Miller KJ, Vansteensel MJ, Aarnoutse EJ, Leijten FSS, Ramsey NF. Neurophysiologic correlates of fMRI in human motor cortex. Hum Brain Mapp 2012;33(7):1689–99.

[22] Schalk G, McFarland DJ, Hinterberger T, Birbaumer N, Wolpaw JR. BCI2000: a general-purpose brain–computer interface (BCI) system. IEEE Trans Bio-Med Eng 2004;51(6):1034–43.

[23] Wilson JA, Mellinger Jr, Schalk G, Williams J. A procedure for measuring latencies in brain–computer interfaces. IEEE Trans Biomed Eng 2010;57(7):1785–97.

[24] Schalk G, Brunner P, Gerhardt LA, Bischof H, Wolpaw JR. Brain–computer interfaces (BCIs): detection instead of classification. J Neurosci Methods 2008;167(1):51–62.

[25] Miller KJ, DenNijs M, Shenoy P, Miller JW, Rao RPN, Ojemann JG. Real-time functional brain mapping using electrocorticography. Neuroimage 2007;37(2):504–7.

[26] Breshears J, Sharma M, Anderson NR, Rashid S, Leuthardt EC. Electrocorticographic frequency alteration mapping of speech cortex during an awake craniotomy: case report. Stereotact Funct Neurosurg 2010;88(1):11–5.

[27] Roland J, Brunner P, Johnston J, Schalk G, Leuthardt EC. Passive real-time identification of speech and motor cortex during an awake craniotomy. Epilepsy Behav 2010;18(1–2):123–8.

[28] Wechsler D. Wechsler adult intelligence scale—fourth edition (WAIS–IV). NCS Pearson: San Antonio, TX; 2008.

[29] Brunner P, Ritaccio AL, Lynch TM, Emrich JF, Wilson JA, Williams JC, et al. A practical procedure for real-time functional mapping of eloquent cortex using electrocorticographic signals in humans. Epilepsy Behav 2009;15(3).

[30] Maes F, Collignon A, Vandermeulen D, Marchal G, Suetens P. Multimodality image registration by maximization of mutual information. IEEE Trans Med Imaging 1997;16(2):187–98.

[31] Hermes D, Miller KJ, Noordmans HJ, Vansteensel MJ, Ramsey NF. Automated electrocorticographic electrode localization on individually rendered brain surfaces. J Neurosci Methods 2010;185(2):293–8.

[32] Gupta D, Hill NJ, Adamo MA, Ritaccio A, Schalk G. Localizing ECoG electrodes on the cortical anatomy without post-implantation imaging. Neuroimage Clin 2014;6:64–76.

[33] Kubanek J, Schalk G. NeuralAct: a tool to visualize electrocortical (ECoG) activity on a three-dimensional model of the cortex. Neuroinformatics 2015;13(2):167–74.

[34] Vansteensel MJ, Bleichner MG, Dintzner LT, Aarnoutse EJ, Leijten FSS, Hermes D, et al. Task-free electrocorticography frequency mapping of the motor cortex. Clin Neurophysiol 2013;124(6):1169–74.

[35] Sinai A, Bowers CW, Crainiceanu CM, Boatman D, Gordon B, Lesser RP, et al. Electrocorticographic high gamma activity versus electrical cortical stimulation mapping of naming. Brain 2005;128(Pt 7):1556–70.

[36] Miller KJ, Abel TJ, Hebb AO, Ojemann JG. Rapid online language mapping with electrocorticography. J Neurosurg Pediatr 2011;7(5):482–90.

[37] Korostenskaja M, Chen P-C, Salinas CM, Westerveld M, Brunner P, Schalk G, et al. Real-time functional mapping: potential tool for improving language outcome in pediatric epilepsy surgery. J Neurosurg Pediatr 2014;1-9.

[38] Su DK, Ojemann JG. Electrocorticographic sensorimotor mapping. Clin Neurophysiol 2013;124(6):1044–8.

[39] Ojemann GA, Fried I, Lettich E. Electrocorticographic (ECoG) correlates of language. I. Desynchronization in temporal language cortex during object naming. Electroencephalogr Clin Neurophysiol 1989;73(5):453–63.

[40] FitzGerald DB, Cosgrove GR, Ronner S, Jiang H, Buchbinder BR, Belliveau JW, et al. Location of language in the cortex: a comparison between functional MR imaging and electrocortical stimulation. AJNR Am J Neuroradiol 1997;18(8):1529–39.

[41] Pouratian N, Bookheimer SY, Rex DE, Martin NA, Toga AW. Utility of preoperative functional magnetic resonance imaging for identifying language cortices in patients with vascular malformations. J Neurosurg 2002;97(1):21–32.

[42] Rutten GJM, Ramsey NF, van Rijen PC, Noordmans HJ, van Veelen CWM. Development of a functional magnetic resonance imaging protocol for intraoperative localization of critical temporoparietal language areas. Ann Neurol 2002;51(3):350–60.

[43] Roux F-E, Boulanouar K, Lotterie J-A, Mejdoubi M, LeSage JP, Berry I. Language functional magnetic resonance imaging in preoperative assessment of language areas: correlation with direct cortical stimulation. Neurosurgery 2003;52(6):1335–45 [discussion 45-7].

[44] Bizzi A, Blasi V, Falini A, Ferroli P, Cadioli M, Danesi U, et al. Presurgical functional MR imaging of language and motor functions: validation with intraoperative electrocortical mapping. Radiology 2008;248(2):579–89.

[45] Giussani C, Roux F-E, Ojemann J, Sganzerla EP, Pirillo D, Papagno C. Is preoperative functional magnetic resonance imaging reliable for language areas mapping in brain tumor surgery? Review of language functional magnetic resonance imaging and direct cortical stimulation correlation studies. Neurosurgery 2010;66(1):113–20.

[46] Rutten GJM, Ramsey NF, van Rijen PC, van Veelen CWM. Reproducibility of fMRI-determined language lateralization in individual subjects. Brain Lang 2002;80(3):421–37.

[47] Freeman WJ, Rogers LJ, Holmes MD, Silbergeld DL. Spatial spectral analysis of human electrocorticograms including the alpha and gamma bands. J Neurosci Methods 2000;95(2):111–21.

[48] Wang W, Degenhart AD, Collinger JL, Vinjamuri R, Sudre GP, Adelson PD, et al. Human motor cortical activity recorded with micro-ECoG electrodes, during individual finger movements. Conference proceedings: Annual International Conference of the IEEE Engineering in Medicine and Biology Society IEEE Engineering in Medicine and Biology Society Conference 2009; 2009. p. 586–9.

[49] Leuthardt EC, Freudenberg Z, Bundy D, Roland J. Microscale recording from human motor cortex: implications for minimally invasive electrocorticographic brain-computer interfaces. Neurosurg Focus 2009;27(1), E10.

[50] Reulen HJ, Schmid UD, Ilmberger J, Eisner W, Bise K. Tumor surgery of the speech cortex in local anesthesia. Neuropsychological and neurophysiological monitoring during operations in the dominant hemisphere. Nervenarzt 1997;68(10):813–24.

[51] Schiffbauer H, Berger MS, Ferrari P, Freudenstein D, Rowley HA, Roberts TPL. Preoperative magnetic source imaging for brain tumor surgery: a quantitative comparison with intraoperative sensory and motor mapping. Neurosurg Focus 2003;15(1), E7.

[52] Sacko O, Lauwers-Cances V, Brauge D, Sesay M, Brenner A, Roux F-E. Awake craniotomy vs surgery under general anesthesia for resection of supratentorial lesions. Neurosurgery 2011;68(5):1192–8 [discussion 8-9].

[53] Shaw E, Arusell R, Scheithauer B, O'Fallon J, O'Neill B, Dinapoli R, et al. Prospective randomized trial of low- versus high-dose radiation therapy in adults with supratentorial low-grade glioma: initial report of a North Central Cancer Treatment Group/Radiation Therapy Oncology Group/Eastern Cooperative Oncology Group study. J Clin Oncol 2002;20(9):2267–76.